

**Ubiquitin-coated nanodiamonds bind to autophagy receptors for entry into the selective autophagy pathway**

Kuang-Kai Liu<sup>1</sup>, Wei-Ru, Qiu<sup>2</sup>, Emmanuel Naveen Raj<sup>2</sup>, Huei-Fang Liu<sup>1</sup>, Hou-Syun Huang<sup>1</sup> Yu-Wei Lin<sup>2</sup>, Chien-Jen Chang<sup>1</sup>, Ting-Hua Chen<sup>1</sup>, Chinpio Chen<sup>3</sup>, Huan-Cheng Chang<sup>4</sup>, Jenn-Kang Hwang<sup>5</sup>, and Jui-I Chao<sup>1,2,\*</sup>

<sup>1</sup>Department and Institute of Biological Science and Technology, National Chiao Tung University, Hsinchu 30068, Taiwan

<sup>2</sup>Institute of Molecular Medicine and Bioengineering, National Chiao Tung University, Hsinchu 30068, Taiwan

<sup>3</sup>Department of Chemistry, National Dong Hwa University, Hualien 97401, Taiwan

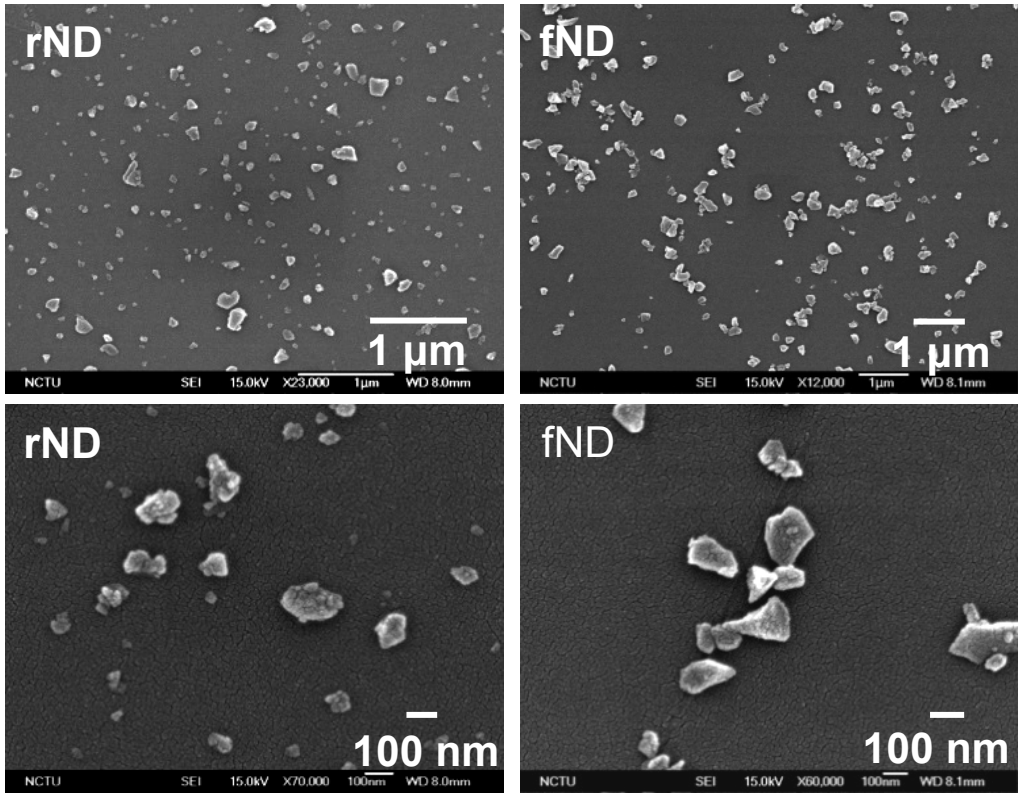
<sup>4</sup>Institute of Atomic and Molecular Sciences, Academia Sinica, Taipei 10672, Taiwan

<sup>5</sup>Institute of Bioinformatics and Systems Biology, National Chiao Tung University, Hsinchu, 30068, Taiwan

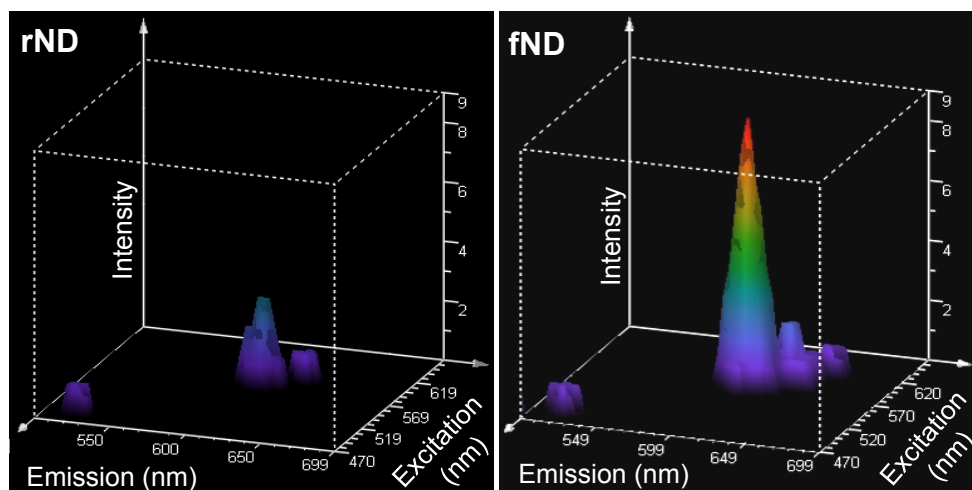
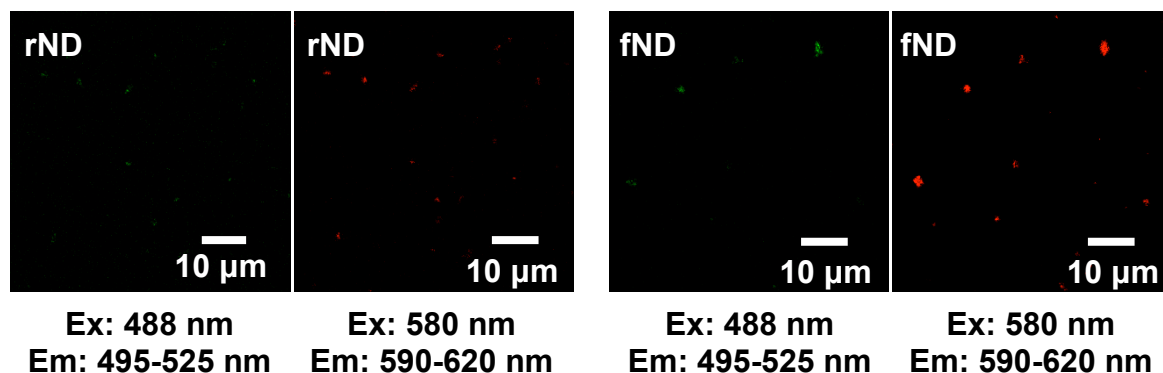
**A**

ND types	Average size (nm)	Zeta potential (mV)
Raw ND (rND)	119.3 ± 33.3	-25.3 ± 1.3
Fluorescent ND (fND)	125.2 ± 33.7	-22.6 ± 0.2

**B**



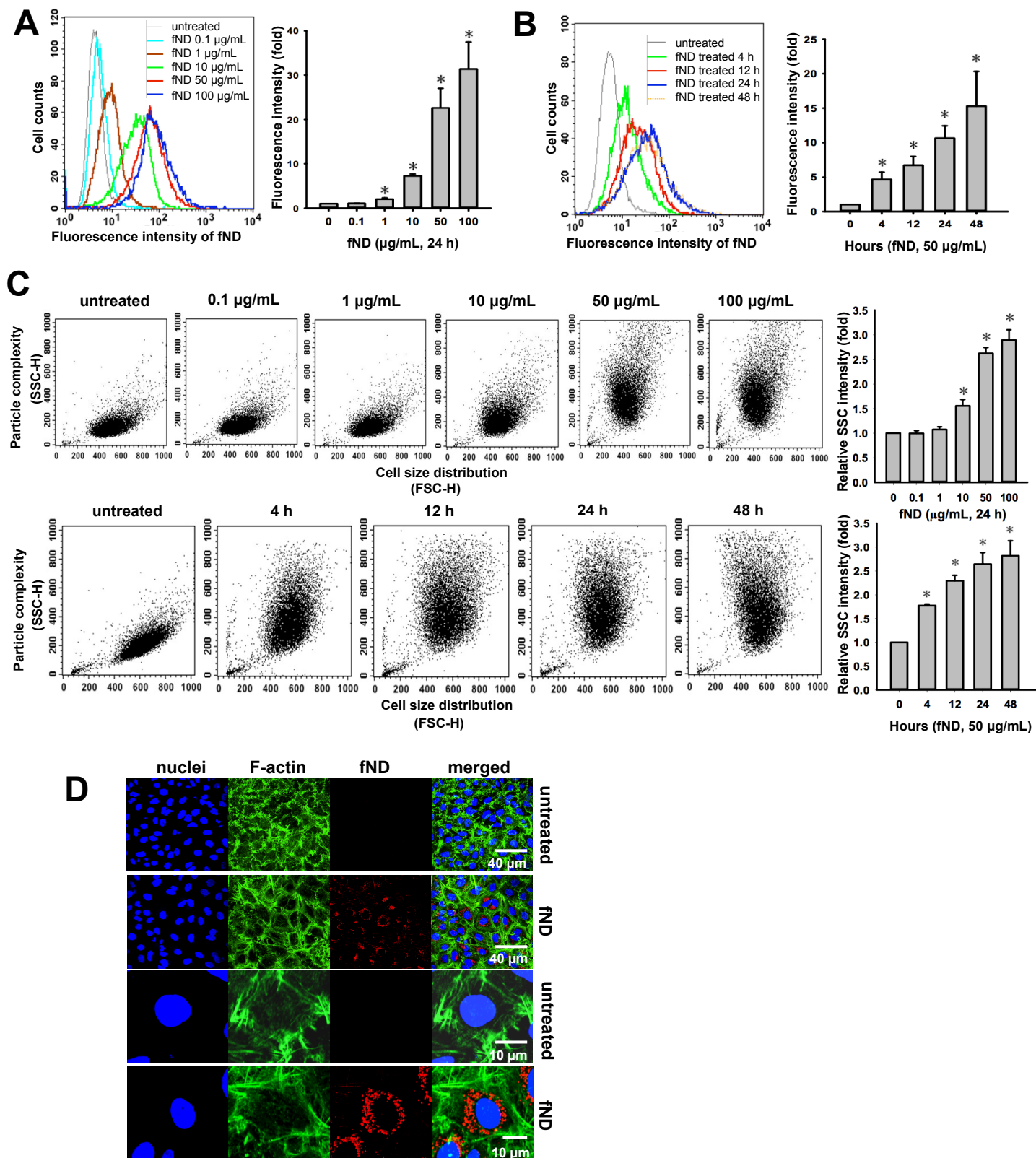
**Figure S1.** Average size and zeta potential of rNDs and fNDs. **(A)** The average sizes of rNDs and fNDs were analyzed by dynamic light scattering (DLS). The concentration of 1-10  $\mu\text{g/mL}$  of rNDs or fNDs in distilled deionized water (DDW) was used for the analysis. The surface charges of nanoparticles were analyzed by zeta potential instrument (Delsa Nano C, Beckman Coulter, USA). **(B)** The concentration of 1  $\mu\text{g/mL}$  rND or fND in DDW was dropped on a silica slide and dried in an electronic dry cabinet. After evaporation at 50°C for 24 h, dried samples were coated with gold and observed by scanning electron microscopy (SEM).

**A****B****C**

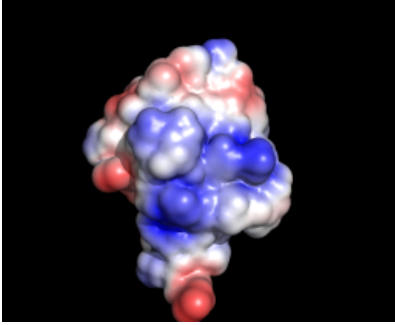
Relative fluorescence intensities	rND	fND
Ex: 488 nm; Em: 495-525 nm (green)	1	1
Ex: 580 nm; Em: 590-620 nm (red)	3.6	10.6

**Figure S2.** The fluorescence intensities of rNDs and fNDs. **(A)** The fluorescence intensities of rND and fND nanoparticles were analyzed using full spectrum scanning by a white light laser of a confocal microscope at the excitation wavelengths from 470 nm to 670 nm (interval of 10 nm) and the emission wavelengths from 500 nm to 700 nm (interval of 20 nm). **(B)** The images of rNDs and fNDs were representative from the fluorescence peaks: the excitation wavelength at 488 nm and the range of emission wavelengths at 495-525 nm, and the excitation wavelength at 580 nm and the range of emission wavelengths at 590-620 nm. **(C)** The relative fluorescence intensities (folds) of rNDs and fNDs were quantified and compared.

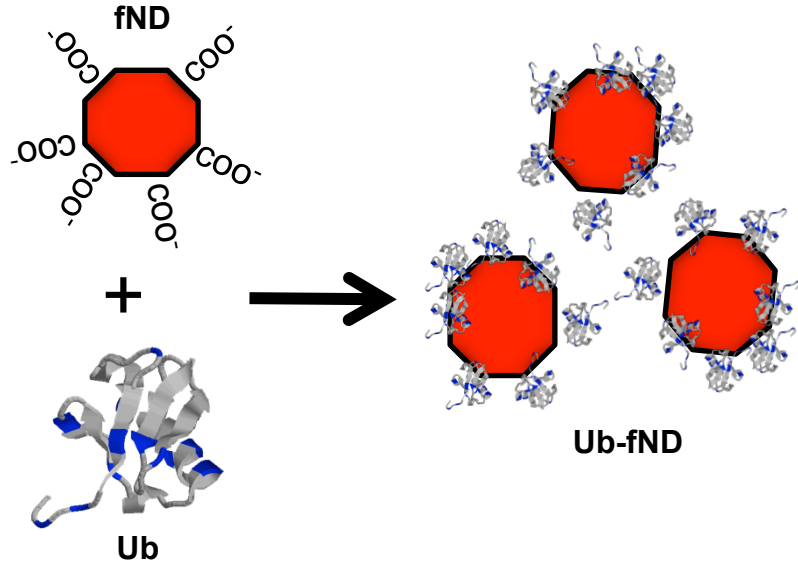




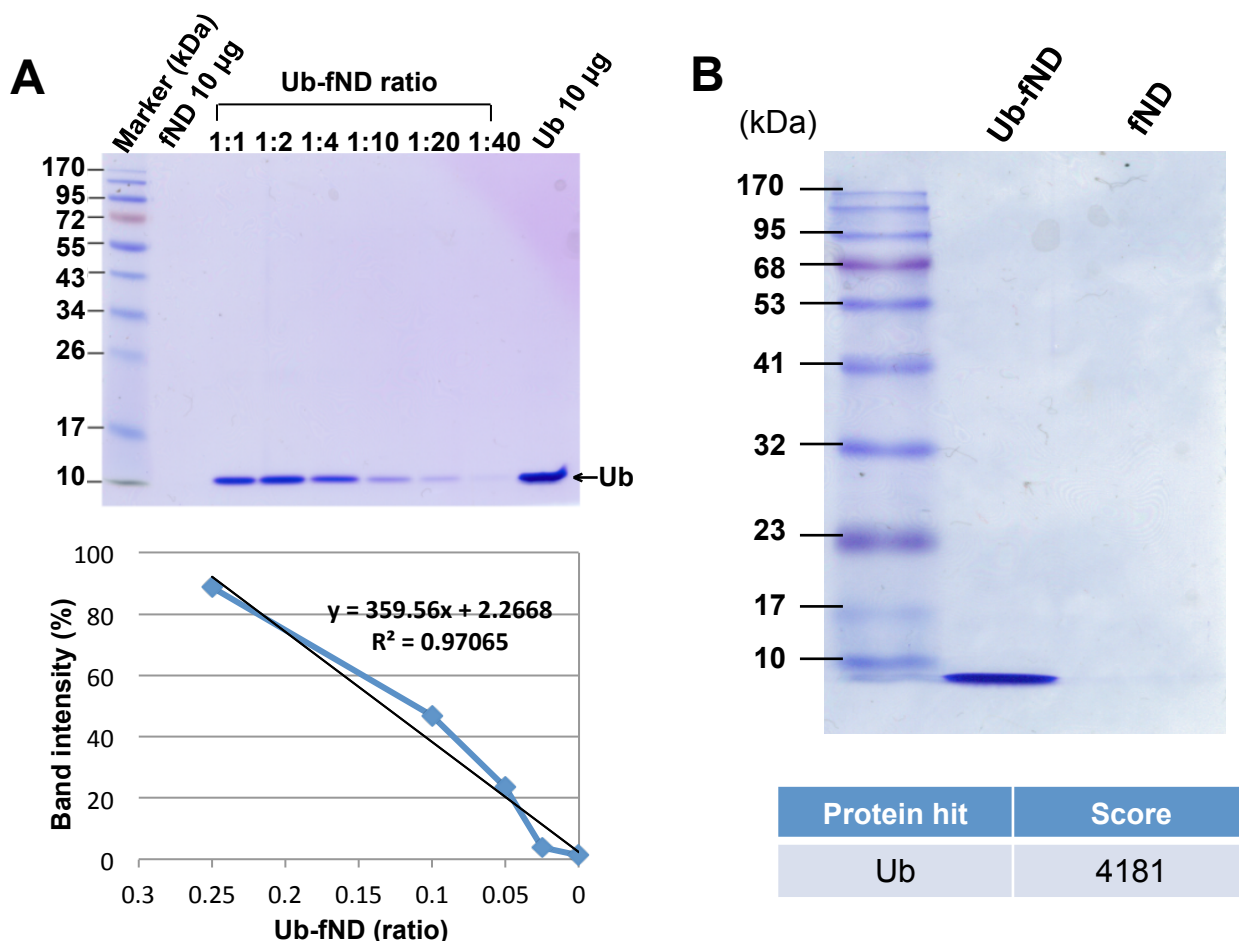
**Figure S3.** The cellular uptake and particle complexity of fND nanoparticles in human cells. (A) A549 cells were treated with or without 0.1-100  $\mu\text{g/mL}$  fNDs for 24 h. (B) A549 cells were treated with or without 50  $\mu\text{g/mL}$  fNDs for 4-48 h. At the end of the treatment, the cells were trypsinized and then subjected to flow cytometer analyses. The fluorescence intensities of fNDs in the cells were quantified using the CellQuest software. (C) The particle complexity (SSC-H) and cell size distribution (FSC-H) were also analyzed by flow cytometer. Results were obtained from 3-4 independent experiments. The bars represent mean  $\pm$  S.E. \*  $p < 0.05$  indicates significant difference between untreated and fND-treated samples. (D) The cells were treated with or without 50  $\mu\text{g/mL}$  fND for 48 h. The fND particles show the red fluorescence by collecting the emission wavelength at 610-750 nm. The cytoskeleton F-actin of the cells was stained with BODIPY FL phalloidin (green). Nuclei were stained with Hoechst 33258 (blue).

**A**

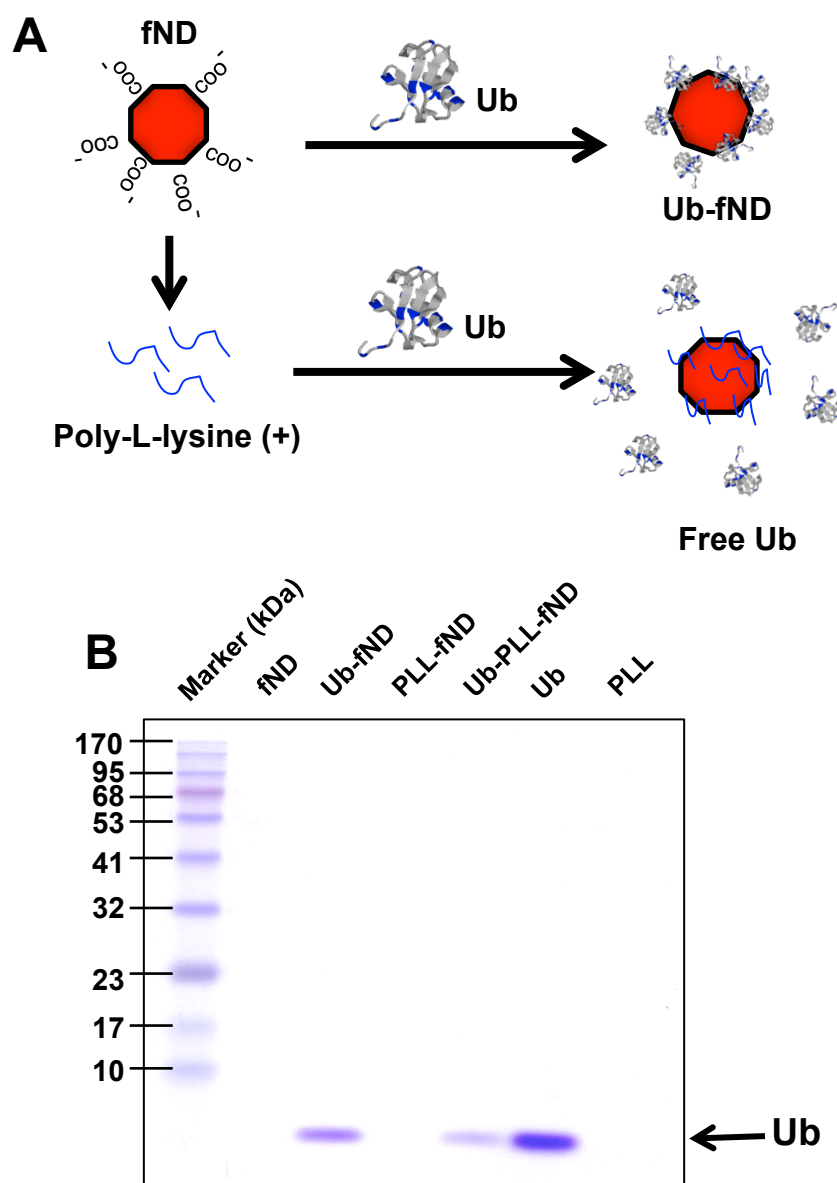
Ubiquitin sequence: (NM\_002954.3)  
 MQIFV**K**TLTG**K**TITLEVEPSDTIENV  
**K**AKIQD**K**EGIPPDQQ**R**LIFAG**K**QLE  
 DGR**T**LSDYNIQ**K**ESTL**H**LV**L****R****L****R**GG

**B**

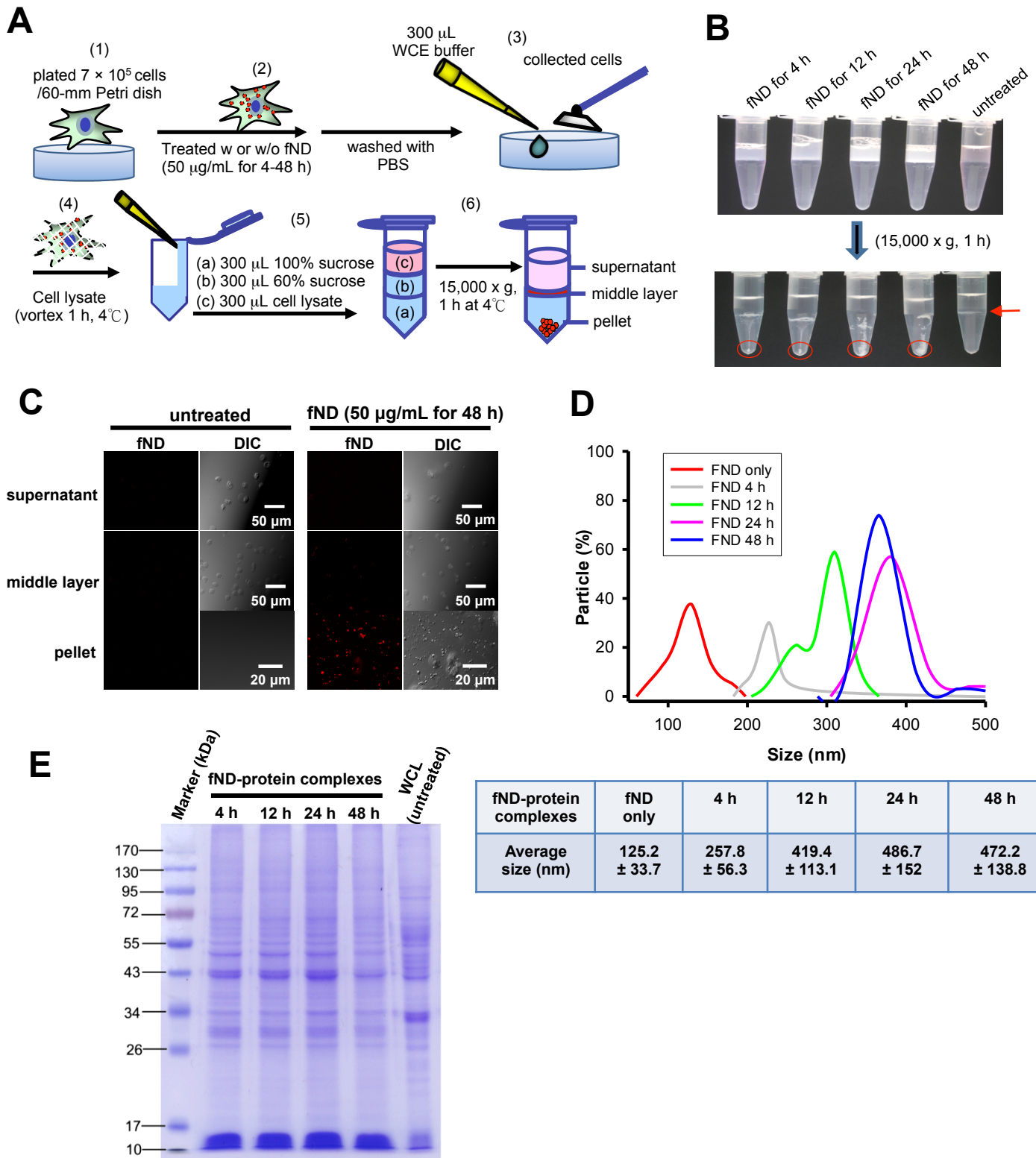
**Figure S4.** The proposed binding model of Ub and fND *in vitro*. **(A)** Schematic model of the sequence and structure of the Ub protein using PyMOL software. The protein sequence of Ub contains basic amino acids, which have a positive charge on arginine (R), lysine (K), and histidine (H). **(B)** Positive charge regions of Ub bind to the negative charge surface of carboxylated fNDs.



**Figure S5.** The binding ratio of Ub and fND *in vitro*. **(A)** The binding levels of Ub on ND nanoparticles were analyzed by SDS-PAGE. After electrophoresis, the gels were stained with Coomassie Brilliant Blue. The ratios of fND and Ub (w/w): 1:1; 1:2; 1:4; 1:10; 1:20; and 1:40 were prepared to analyze their binding affinity. The quantification of band intensities on the SDS-PAGE gel was calculated for the binding affinity of Ub and fND (down panel). **(B)** The ratio of Ub and fND (w/w, 2.5:10) was prepared for Ub protein identification. The Ub bands on the gel were collected and analyzed by Quadrupole time-of-flight mass spectrometer (Q-TOF-MS). The score number shows the identification of Ub.

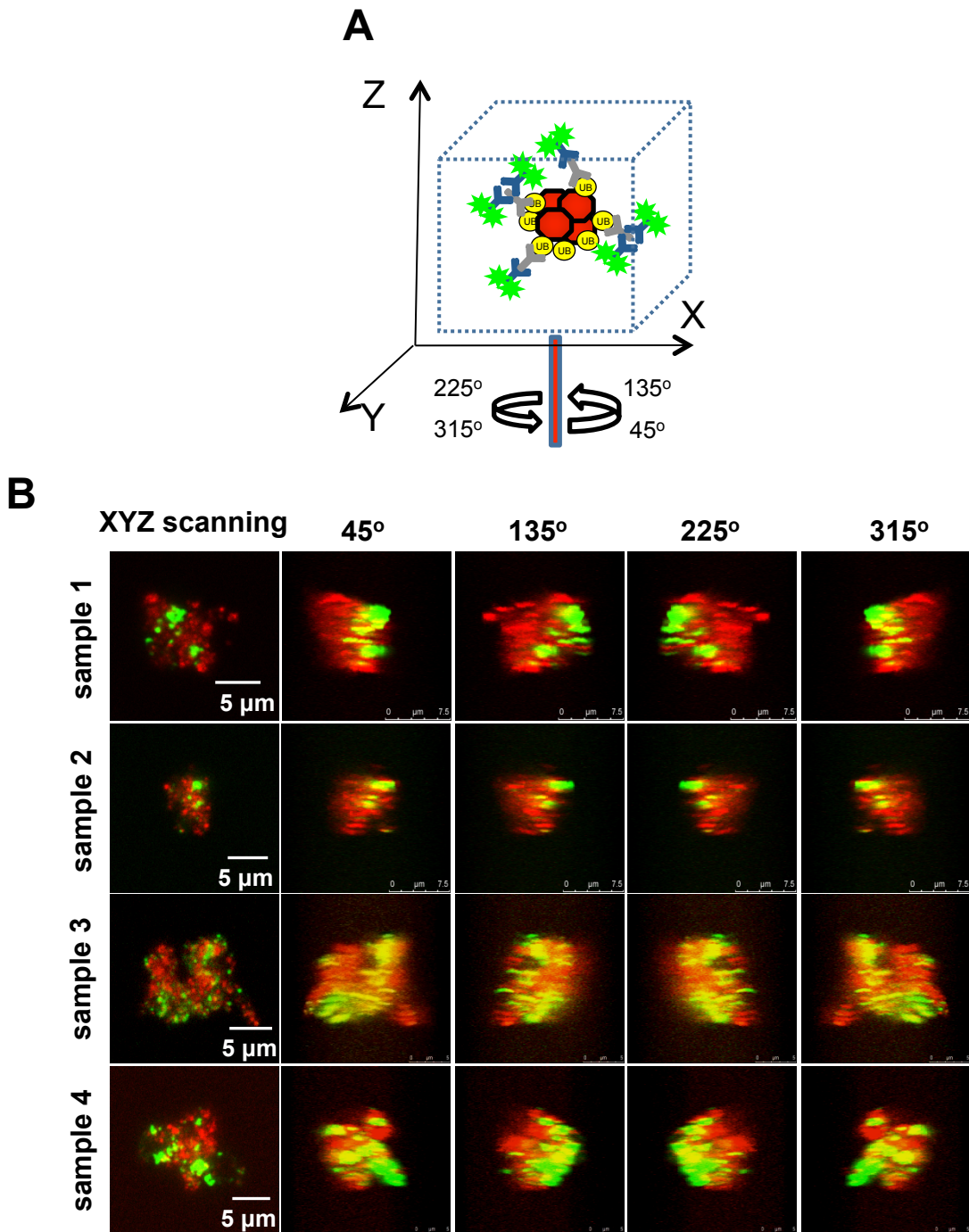


**Figure S6.** Coating of poly-L-lysine (PLL) on fND inhibits the binding of Ub on the fND nanoparticles. **(A)** Schematic model shows the positive charge of PLL suppresses the binding of Ub and fND. **(B)** The binding levels of Ub and fND were examined by SDS-PAGE analysis and Coomassie Brilliant Blue staining. The arrow indicates the bands of Ub. The protein bands in the left indicate the molecular mass of the protein marker.

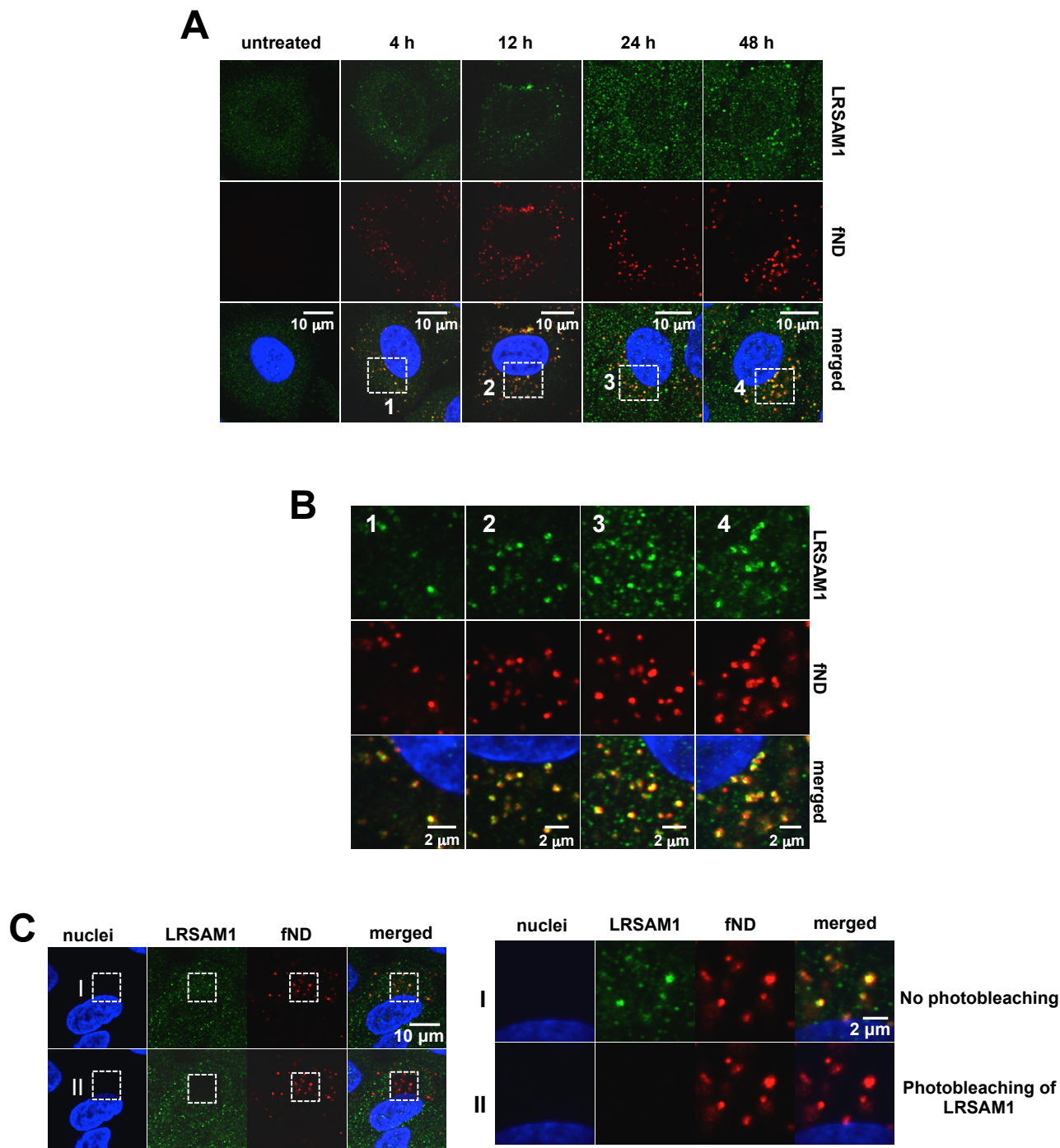


**Figure S7.** The separation of ND-protein complexes in the cells by modified sucrose gradient centrifugation. **(A)** Illustration of fND-protein complexes separated by a modified sucrose gradient centrifugation. **(B)** The A549 cells were left treated with fND (50  $\mu\text{g/mL}$  for 4-48 h). The cell lysates were loaded into the sucrose gradient in centrifuge tubes (upper panel). After centrifugation, the fND-protein complexes were in the bottom of the centrifuge tubes (denoted by red circles). **(C)** Representative confocal microscopy images show the fND-protein complexes. The red color indicates the location of fND particles. DIC, differential interference contrast. **(D)** The size distribution of fND-protein complexes from various time points was analyzed by DLS. **(E)** The fND-protein complexes separated from the cells were analyzed by SDS-PAGE analysis. The whole cell lysate (WCL) indicates the ND-untreated samples. After electrophoresis, the gels were stained with Coomassie Brilliant Blue. The representative data were shown from 1 of 3 independent experiments with similar findings.

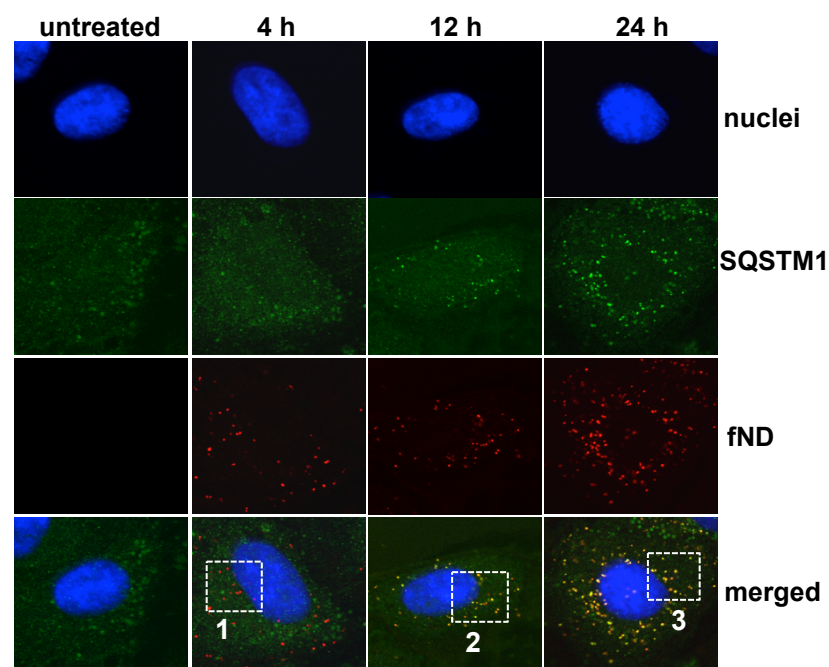
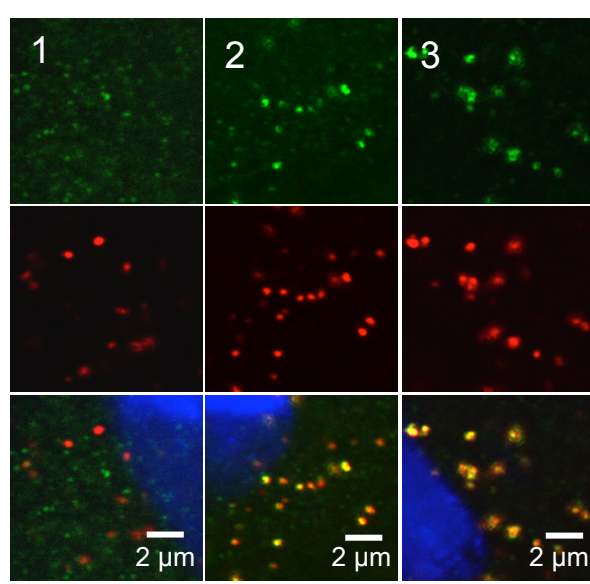
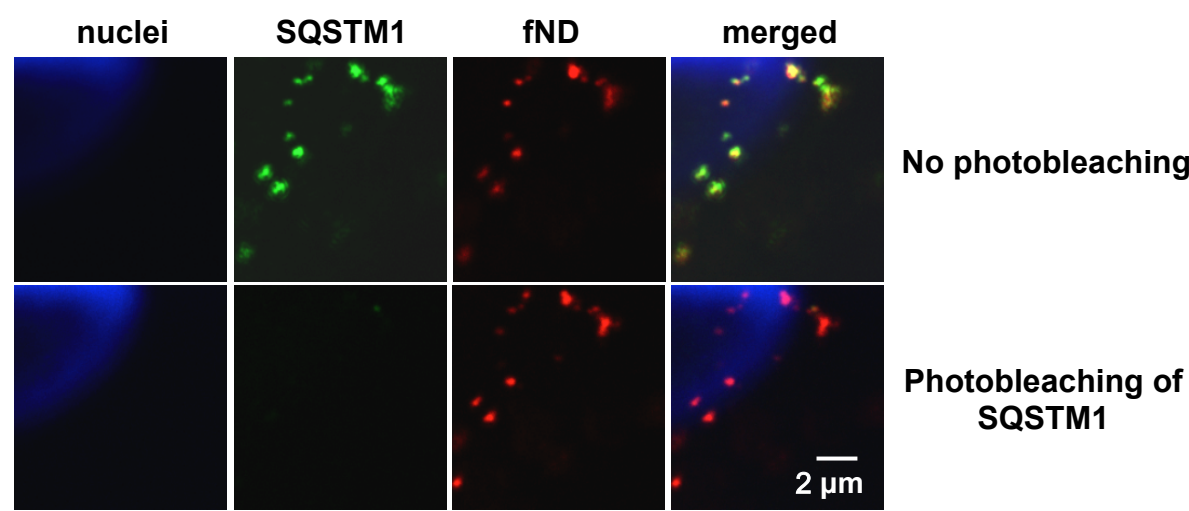




**Figure S8.** Three-dimensional images of Ub K48 binding on the fND nanoparticles in the fND-protein complexes. (A) Schematic model illustrates the fND-protein complexes in the 3-dimensional scanning by confocal microscopy. (B) A549 cells were treated with fNDs (50  $\mu\text{g/mL}$  for 24 h). The fND-protein complexes in the cells were separated and incubated with rabbit anti-Ub K48 and then stained with goat anti-rabbit Hylite 488. Green fluorescence shows the location of Ub K48. Red color shows the location of fND particles, which excited with wavelength 580 nm and the emission was collected in the range of 610-750 nm. The angle rotation of 45°, 135°, 225° and 315° is shown from 4 samples. Each sample was merged from 25-30 images by 3-dimensional scanning (left side images).



**Figure S9.** LRSAM1 E3 ligase interacts with fNDs in cells. (A) A549 cells were treated with or without FND (10  $\mu\text{g/mL}$  for 4-48 h). The cells were incubated with rabbit anti-LRSAM1 and then incubated with goat anti-rabbit Hylite 488. Green color indicates the location of LRSAM1. Red color indicates the location of fND particles, which excited with wavelength 580 nm and the emission was collected in the range of 610-750 nm. The nuclei were stained with Hoechst 33258 (blue). (B) The magnified pictures were from the marked regions 1-4 of (A). Yellow color shows the colocalization of LRSAM1 and fNDs. (C) Identification of LRSAM1 location on fNDs by laser photobleaching. A549 cells were treated with fNDs (10  $\mu\text{g/mL}$  for 24 h). I and II were magnified from the marked rectangles of the left panels. Rectangle II was exposed to high laser power at 488 nm for 10 sec. After high laser power excitation for 10 sec, the green fluorescence of LRSAM1 was disrupted.

**A****B****C**

**Figure S10.** SQSTM1 binds with fND in cells. **(A)** Representative confocal microscopy images of A549 cells left untreated or treated with fNDs (10  $\mu\text{g/mL}$  for 4-24 h) show the location of SQSTM1 (green) and fNDs (red). The cells were incubated with rabbit anti-SQSTM1 and then incubated with goat anti-rabbit Hylite 488. The nuclei were stained with Hoechst 33258 (blue). **(B)** Magnified images of the regions marked by white boxes 1-3 in **(A)** show the colocalization of SQSTM1 and fND particles (yellow). **(C)** Confocal microscopy images of laser photobleaching show the identification of SQSTM1 location on fNDs. After being exposed to high laser power at 488 nm for 10 sec, the green fluorescence of SQSTM1 was disrupted (lower panel).



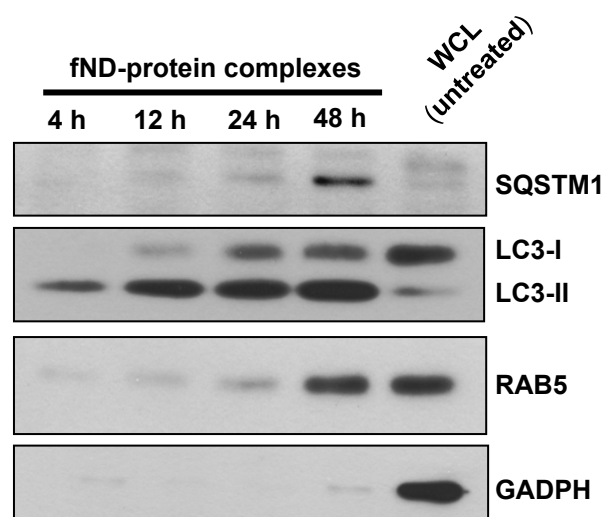


**Figure S11.** Identification of SQSTM1, LC3 and RAB5 proteins in the fND-protein complexes in normal lung fibroblast. HFL-1 cells were left untreated or treated with fND (50  $\mu\text{g}/\text{mL}$  for 4-48 h). At the end of treatment, the fND-protein complexes in the cells were separated by a sucrose gradient centrifugation method as described. SQSTM1, LC3, RAB5 and GAPDH protein levels in the fND-protein complexes were analyzed by western blot using specific antibodies. WCL shows the fND-untreated samples.

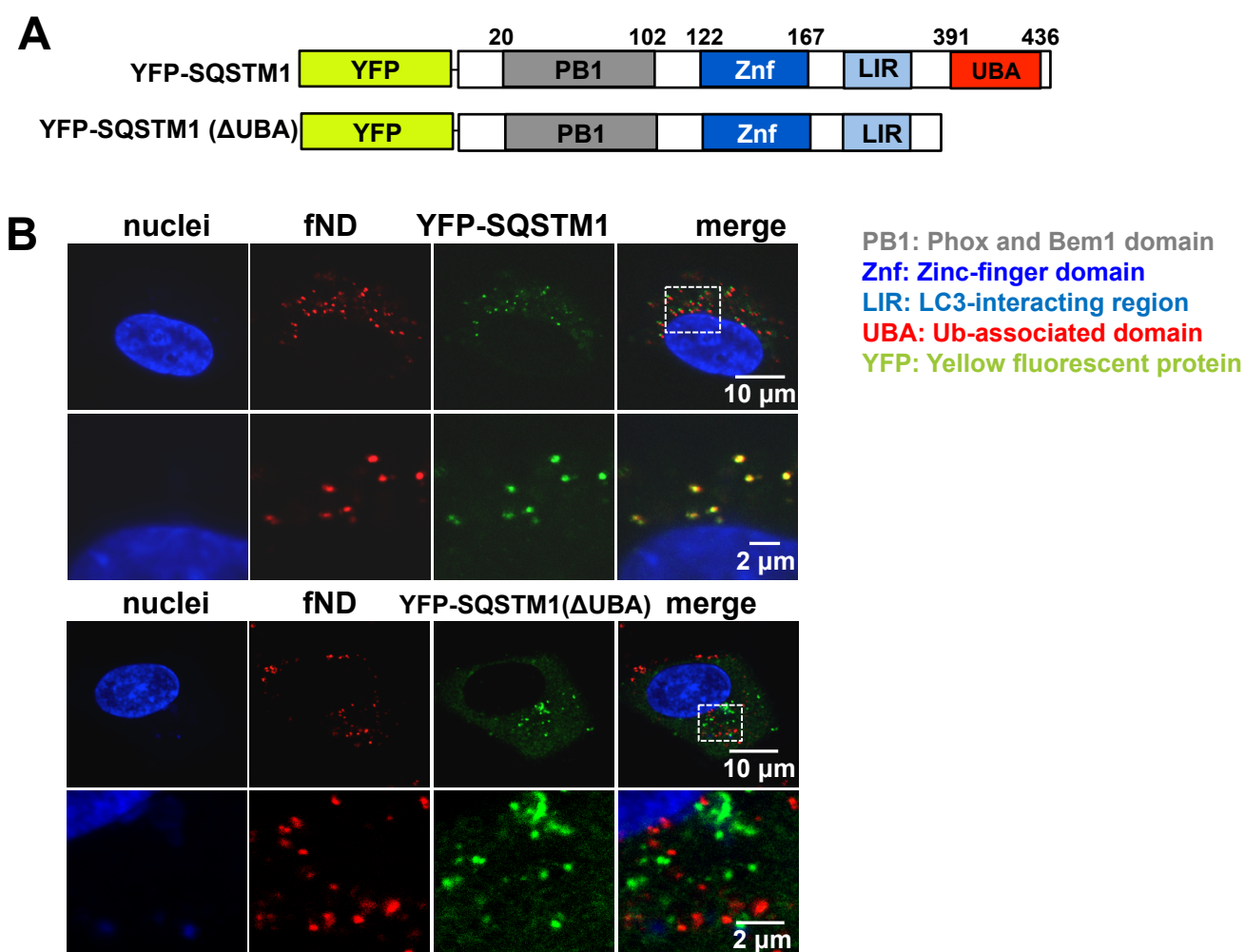


**Figure S12.** Ectopically expressed wild-type YFP-SQSTM1 can bind to fNDs in cells. **(A)** Schematic illustration of wild-type YFP-SQSTM1 and mutant YFP-SQSTM1 ( $\Delta$ UBA) protein structures. The cDNA fragment was cloned into the pcDNA 3.1(+) vector (Invitrogen, V79020). Wild-type SQSTM1 plasmid can express the Ub-associated domain (UBA) whereas the mutant SQSTM1 ( $\Delta$ UBA) plasmid express a UBA-deleted form of SQSTM1. **(B)** Representative images from the Multiphoton and Confocal Microscope System of A549 cells transfected with wild-type SQSTM1 plasmids or mutant SQSTM1 ( $\Delta$ UBA) plasmids that were treated with fNDs (10  $\mu$ g/mL for 24 h), showing the location of SQSTM1 (green) and fND particles (red). The nuclei were stained with Hoechst 33258 (blue). The colocalization of SQSTM1 and fND particles is shown (yellow).

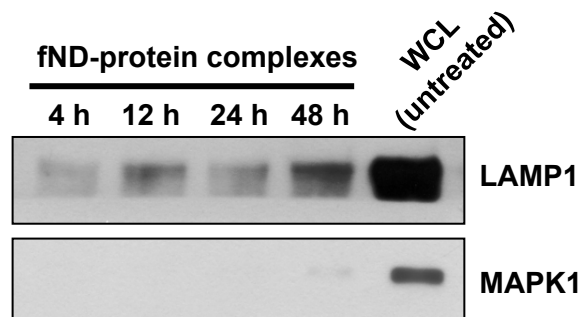


**Figure S13.** Identification of LAMP1 proteins in the fND-protein complexes in normal lung fibroblast. HFL-1 cells were left untreated or treated with fND (50  $\mu\text{g/mL}$  for 4-48 h). At the end of treatment, the fND-protein complexes in the cells were separated by a sucrose gradient centrifugation method as described. LAMP1 and MAPK1/ERK2 protein levels in the fND-protein complexes were analyzed by western blot using specific antibodies. WCL shows the fND-untreated samples.

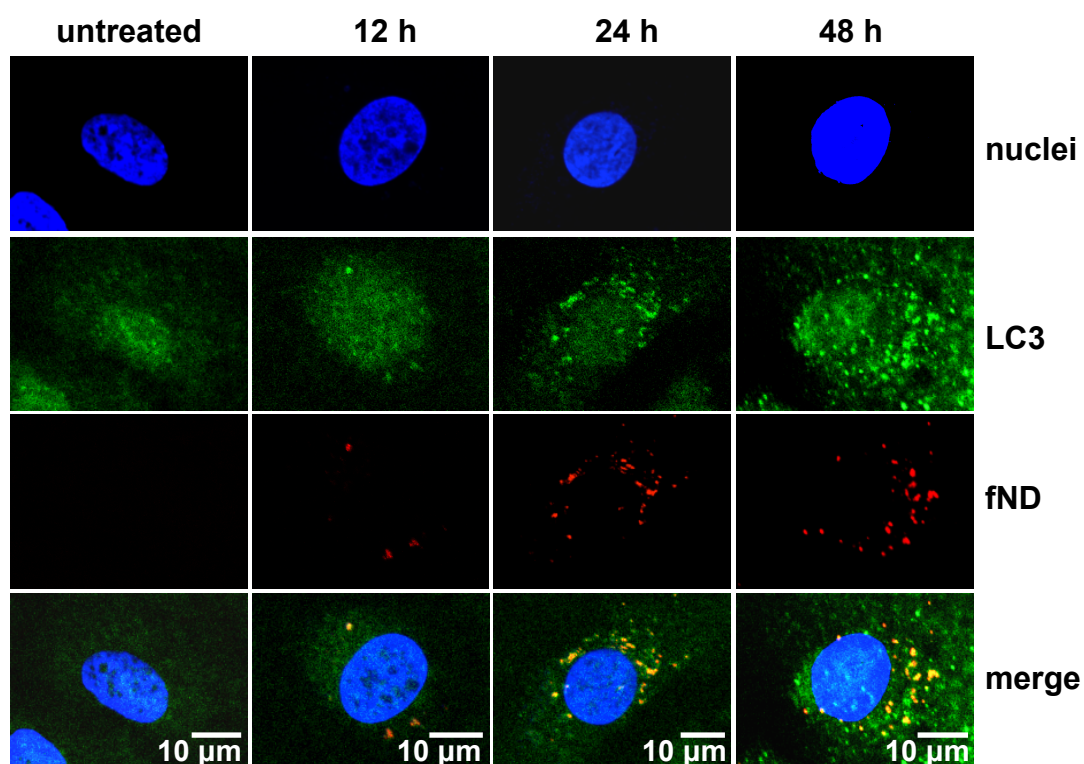


**Figure S14.** Accumulation of fNDs in autophagosomes in a time-dependent manner. Representative confocal microscopy images of A549 cells untreated or treated with fNDs (10  $\mu$ g/mL for 12-48 h) show the location of LC3 (green) and fND particles (red). The nuclei were stained with Hoechst 33258 (blue). The colocalization of LC3 and fND particles is shown (yellow).

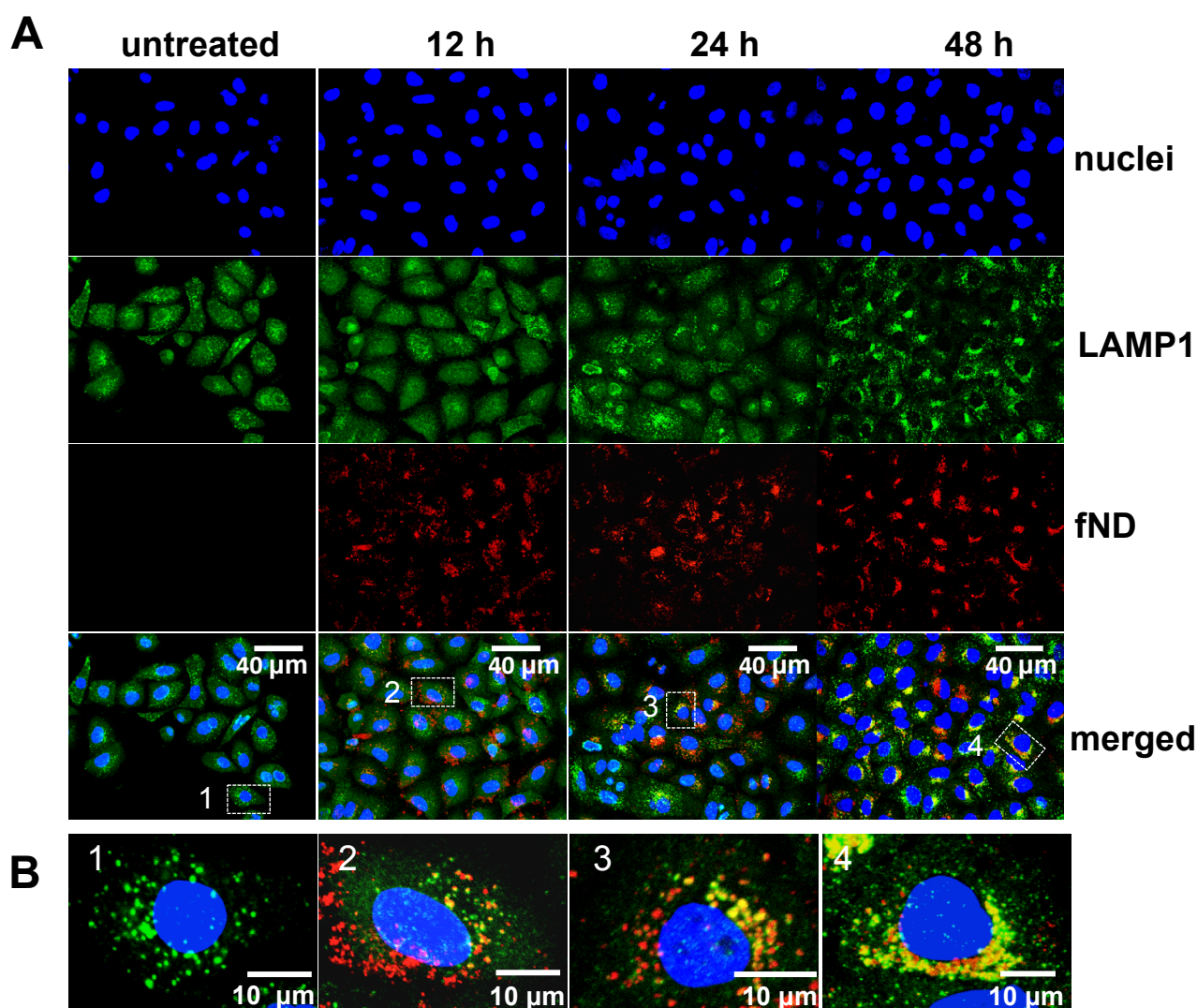


**Figure S15.** Accumulation of fNDs in lysosomes in a time-dependent manner. (A) A549 cells were left untreated or treated with fNDs (10  $\mu\text{g/mL}$  for 12-48 h). Representative confocal microscopy images show the location of LAMP1 (green) and fND particles (red). The nuclei were stained with Hoechst 33258 (blue). The images of (B) were magnified from the regions marked by white boxes 1-4 in (A). Yellow color shows the colocalization of LAMP1 and fND particles.

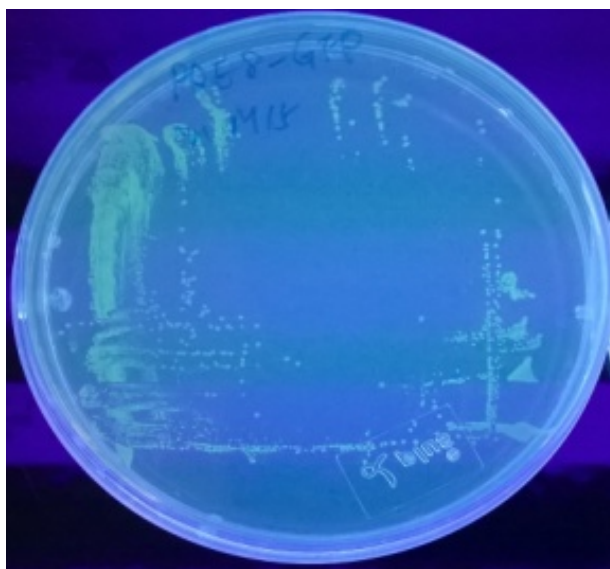


**Figure S16.** Colonies of *E. coli* (pQE 8-GFP) in M15 on an agar plate. The bacteria were cultured on an agar plate. After 24 h incubation, the plate was exposed to UV light. The colonies of *E. coli* were expressing green fluorescence.

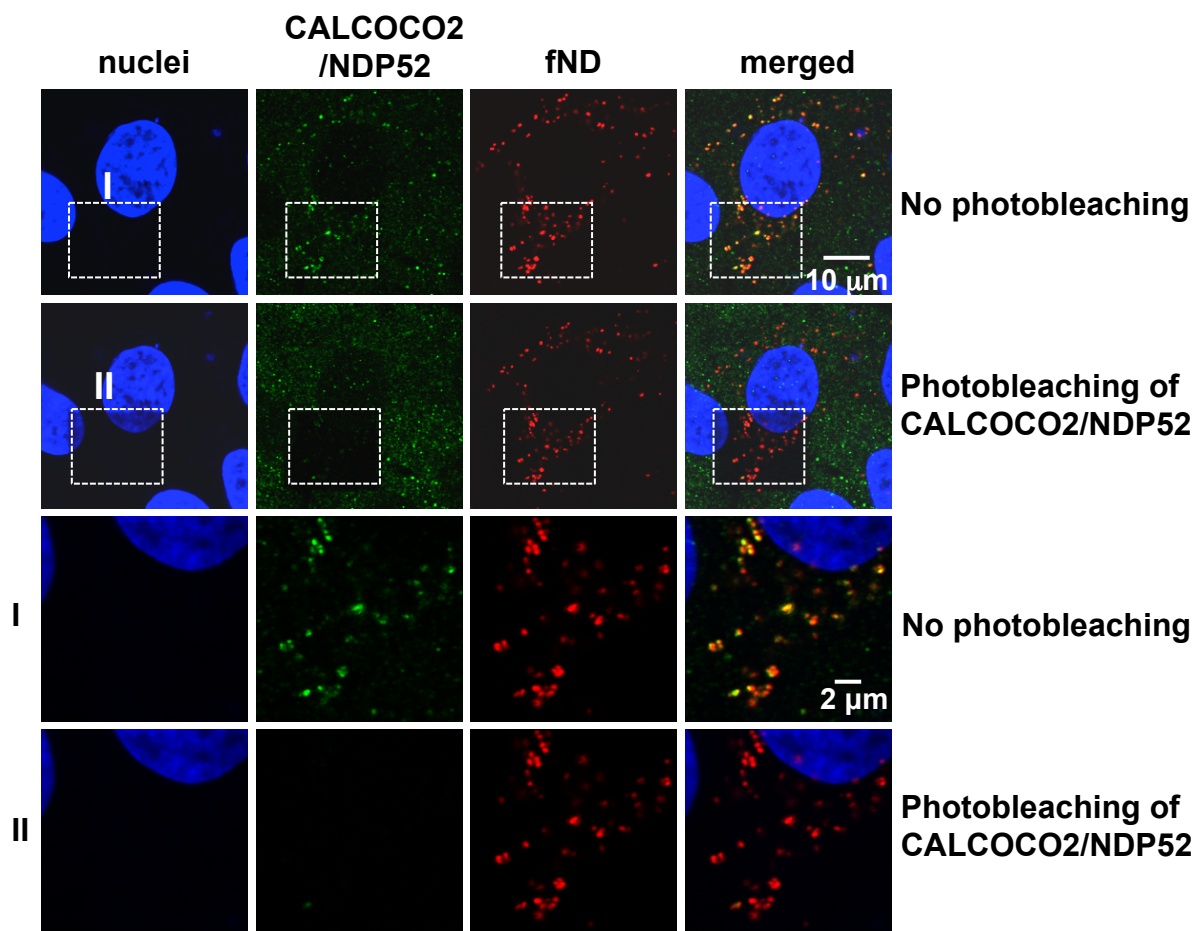


**Figure S17.** Identification of CALCOCO2/NDP52 location on fNDs by laser photobleaching. A549 cells were left treated with fNDs (10  $\mu\text{g/mL}$  for 24 h). At the end of treatment, the cells were incubated with rabbit anti-CALCOCO2/NDP52 and then incubated with goat anti-rabbit Hylite 488. Green color shows the location of CALCOCO2/NDP52. Red color indicates the location of fND particles. The nuclei were stained with Hoechst 33258 (blue). The colocalization of CALCOCO2/NDP52 and fND is shown (yellow). **I** and **II** images were magnified from the regions marked by white boxes (upper panels). White boxed region **II** shows the green fluorescence of CALCOCO2/NDP52 was disrupted (lower panel) after exposure to high laser power at 488 nm for 10 sec.



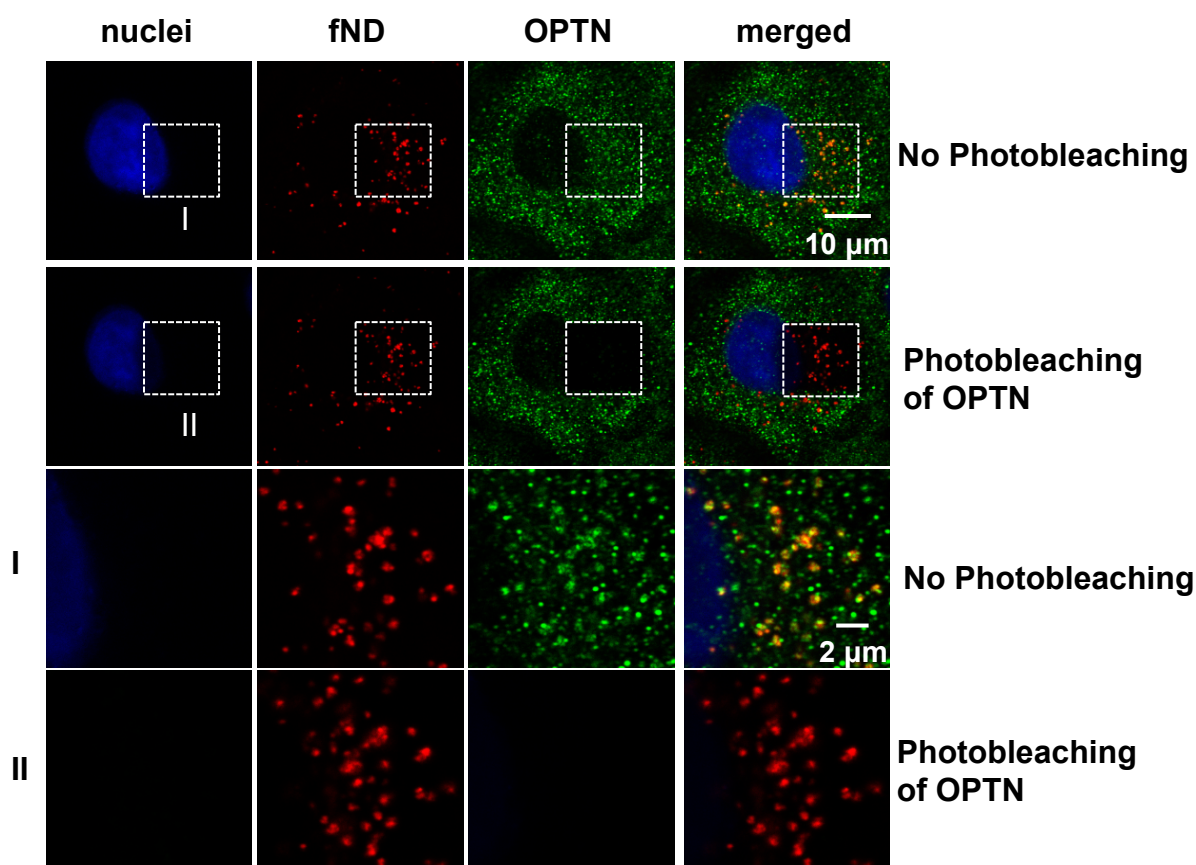


**Figure S18.** Identification of OPTN location on ND by laser photobleaching. A549 cells were left treated with fNDs (10  $\mu\text{g/mL}$  for 24 h). At the end of treatment, the cells were incubated with rabbit anti-OPTN and then incubated with goat anti-rabbit Hylite 488. Green color shows the location of OPTN. Red color indicates the location of fND particles. The nuclei were stained with Hoechst 33258 (blue). The colocalization of OPTN and fND is shown (yellow). **I** and **II** images were magnified from the regions marked by white boxes (upper panels). White boxed region **II** shows the green fluorescence of OPTN was disrupted (lower panel) after exposure to high laser power at 488 nm for 10 sec.



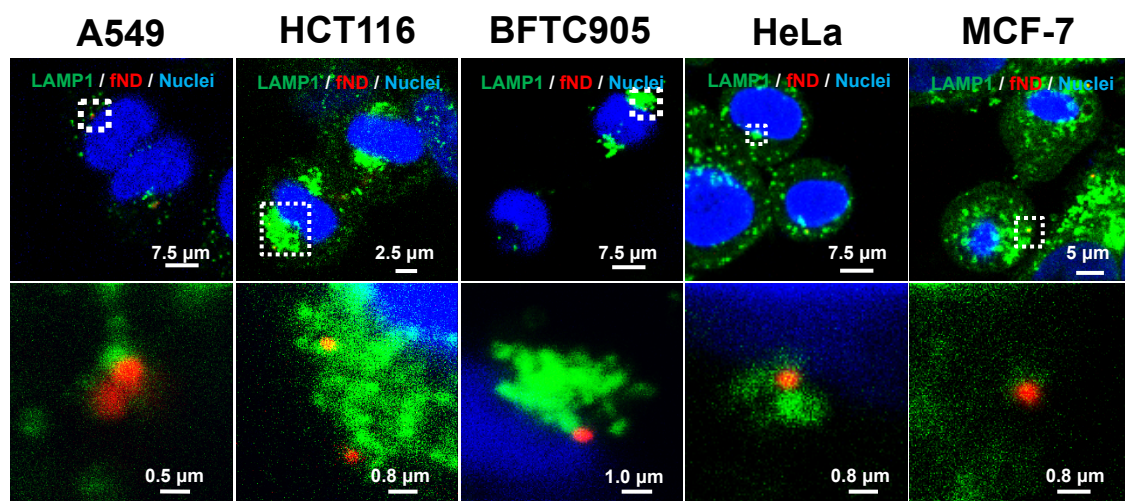


**Figure S19.** Distribution and intracellular localization of fND particles in lysosomes in various human cell types during mitosis after being re-cultured for several days. Representative confocal microscopy images of various cells types were left treated with 50  $\mu\text{g/mL}$  fND particles for 24 h. At the end of treatment, the cells were re-cultured in fresh medium for 2-10 days, showing the location of LAMP1 (green) and fND particles (red). The nuclei were stained with Hoechst 33258 (blue).

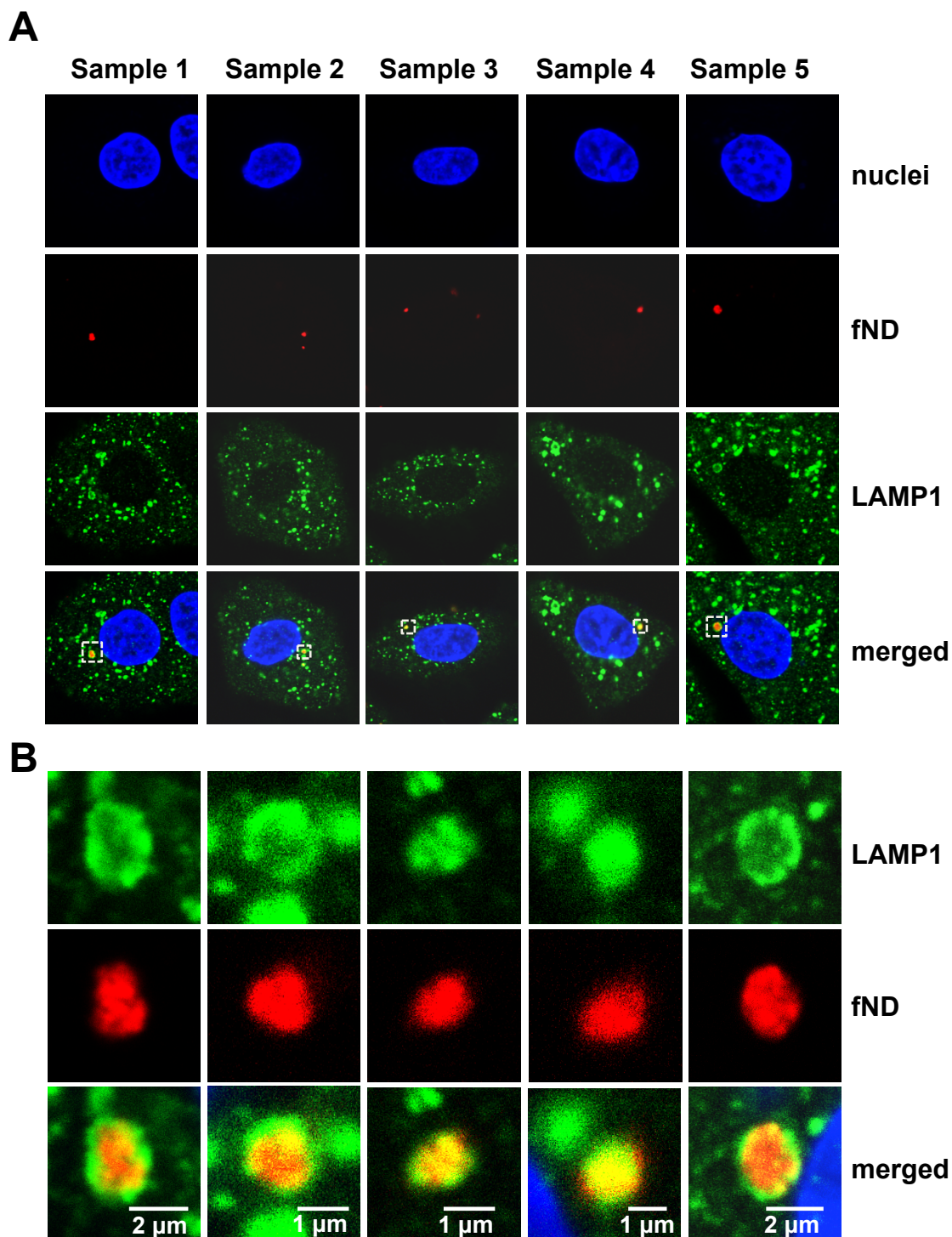


**Figure 20.** Single fND clusters location in lysosomes after re-culturing for 10 days. After treatment with fND particles (50  $\mu\text{g/mL}$  for 48 h), A549 cells were re-cultured in fresh medium for long-term examination every 2 days until 10 days and observed by confocal microscopy analysis. **(A)** Representative confocal microscopy images show the location of LAMP1 (green) and fND particles (red). The nuclei were stained with Hoechst 33258 (blue). **(B)** The images were magnified from the regions marked by white boxes, showing the colocalization of LAMP1 and fND particles (yellow).

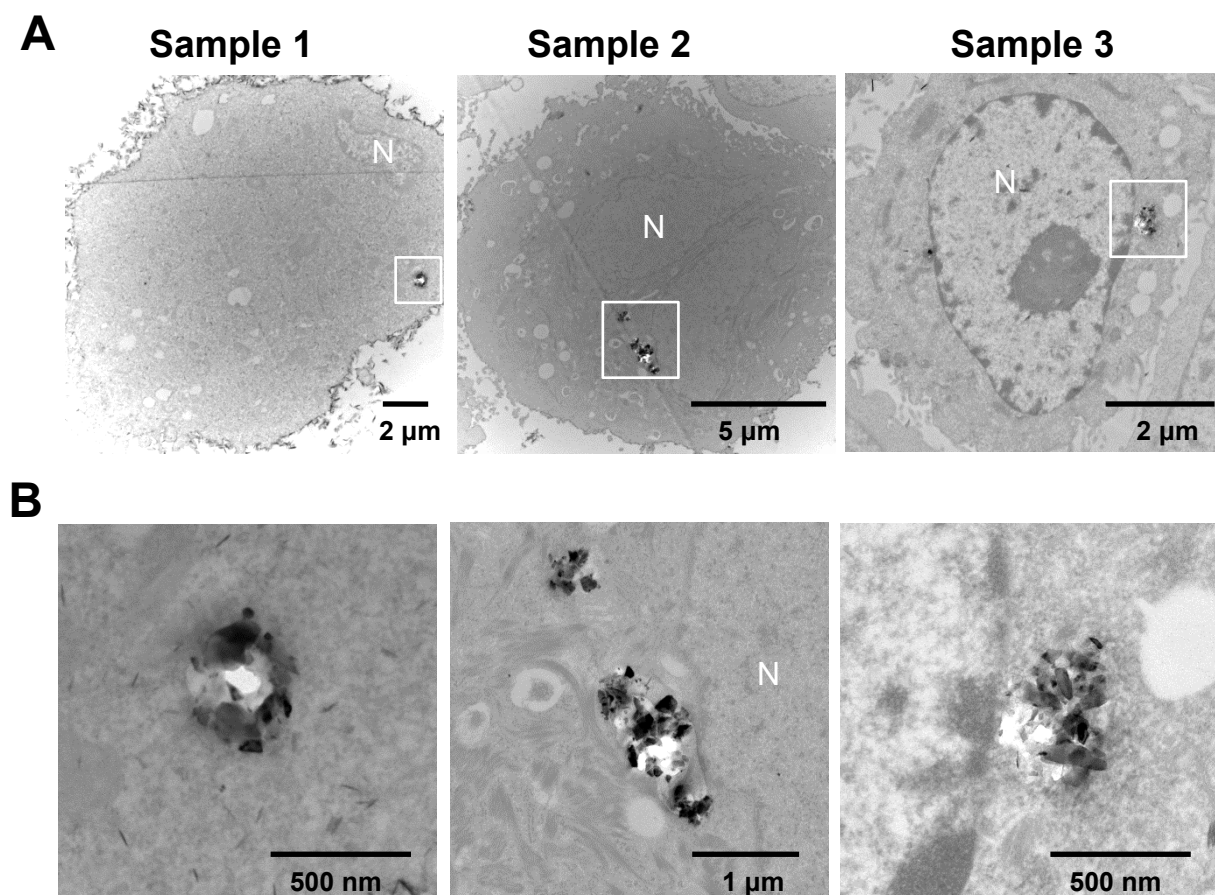


**Figure S21.** The fND clusters locate in vesicles in the cytoplasm. **(A)** A549 cells were left treated with fNDs (50  $\mu\text{g/mL}$  for 4 h). TEM images show the intracellular distribution of fND clusters from 3 independent samples. **(B)** The images were magnified from the regions marked by white boxes in **(A)**. The fND clusters located inside vesicles in the cytoplasm. N indicates the location of nuclei.

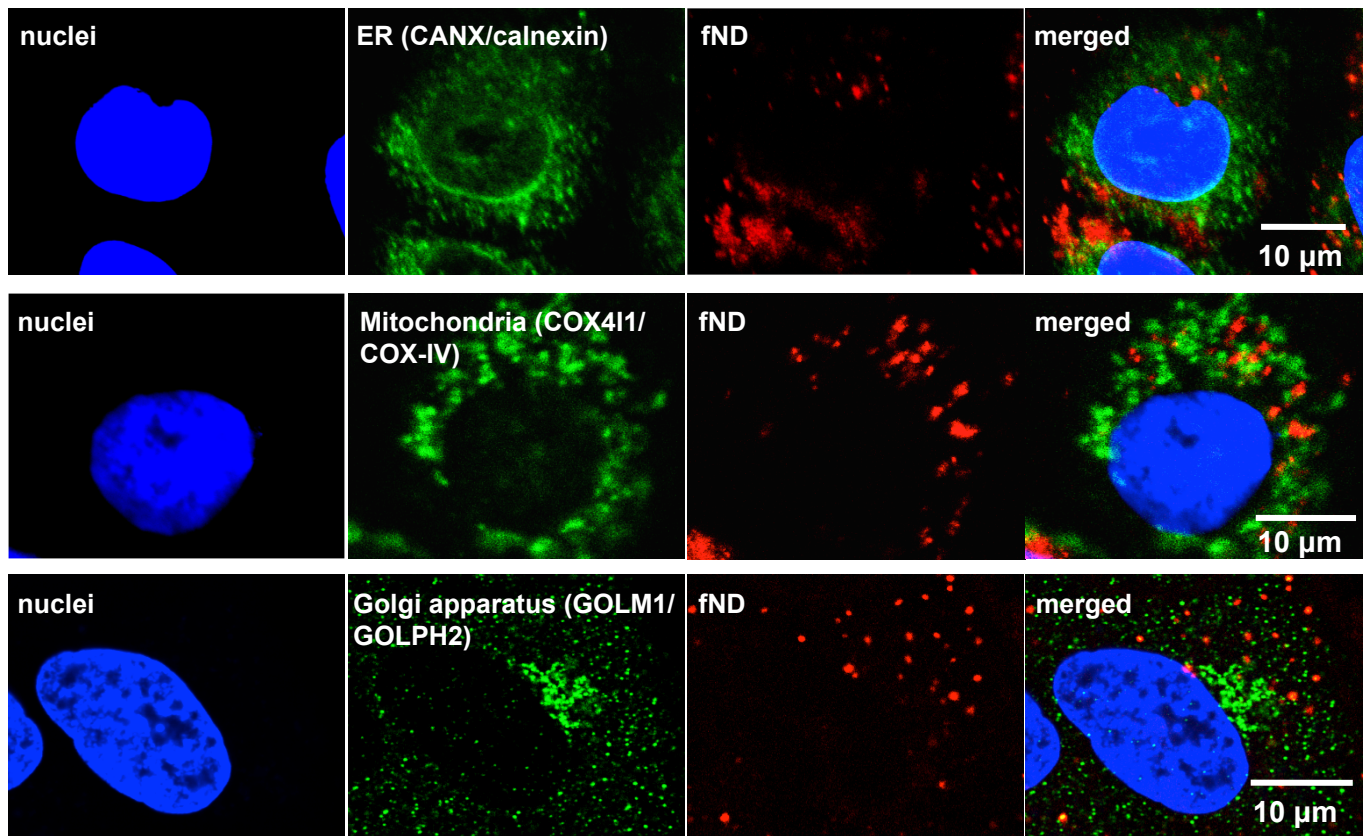


**Figure S22.** fND particles do not locate in the endoplasmic reticulum, mitochondria or Golgi apparatus. A549 cells were left treated with fND (10  $\mu\text{g/mL}$  for 24 h). At the end of treatment, the cells were subjected to nuclei and other organelle staining (green color indicates the location of the endoplasmic reticulum [ER], mitochondria and Golgi apparatus by incubating with rabbit anti-CANX/calnexin [ER marker protein], rabbit anti-COX4I1/COX-IV [mitochondria marker protein] and rabbit anti-GOLM1/GOLPH2 [Golgi apparatus marker protein], respectively), and then incubated with goat anti-rabbit Hylite 488. Red color shows the location of fND particles. Nuclei were stained with Hoechst 33258 (blue).

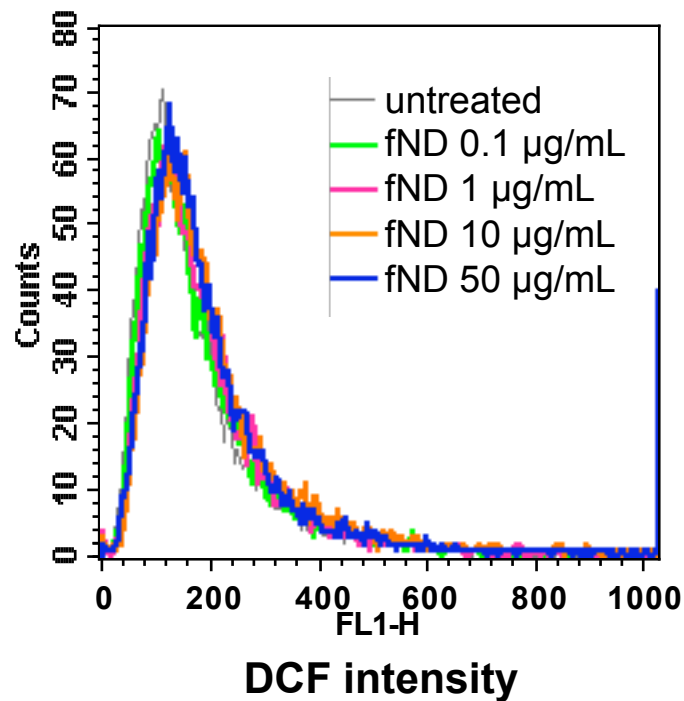


**Figure S23.** fNDs did not increase the free radical levels of cells. A549 cells were left treated with or without 0.1–50  $\mu\text{g/mL}$  fNDs for 24 h. At the end of treatment, the ROS levels in the cells were detected with  $\text{H}_2\text{DCFDA}$  (Calbiochem, 287810) and subjected to flow cytometer analysis. The ROS levels were determined by the production of DCF fluorescence intensity in the cells.



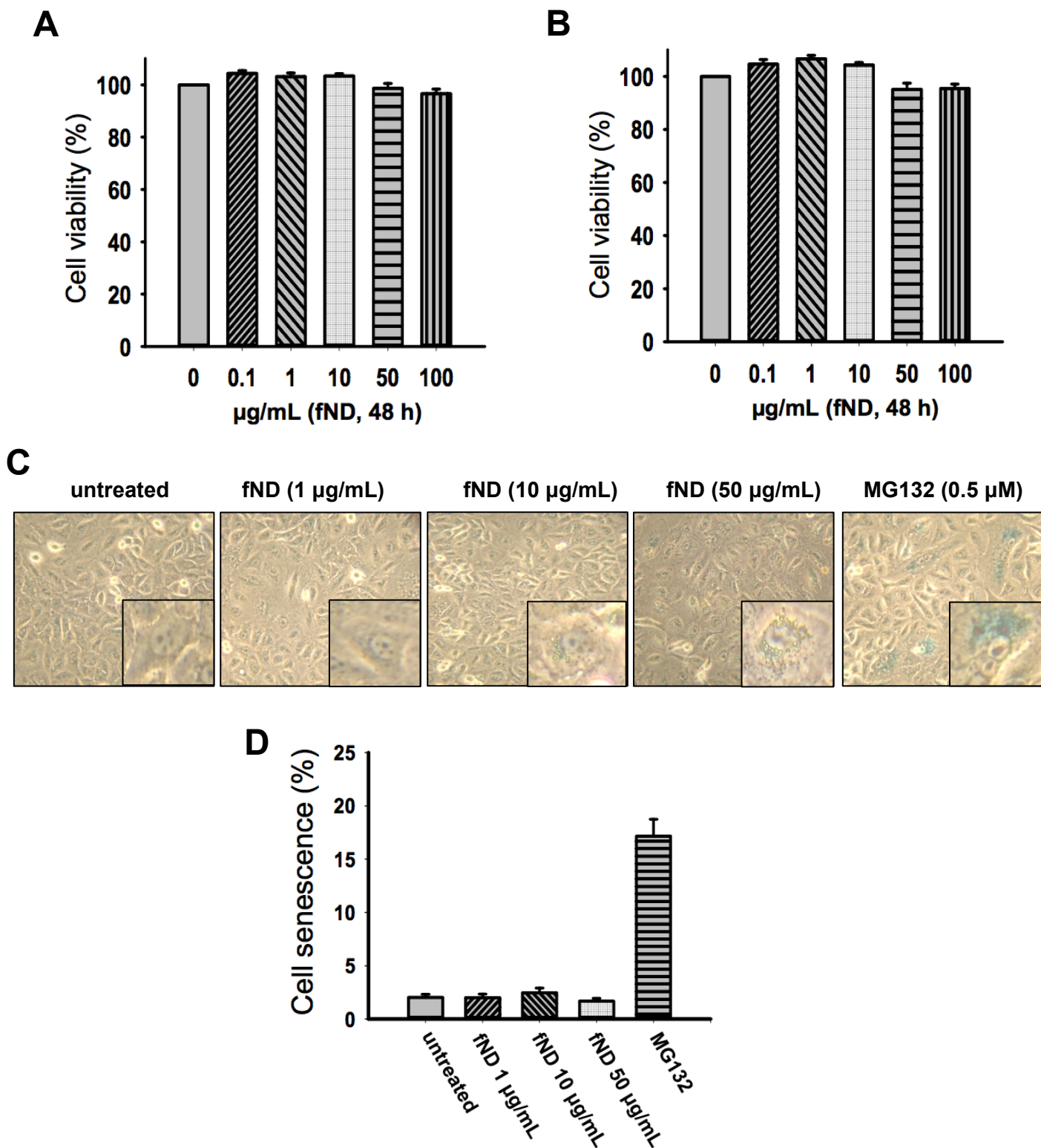


**Figure S24.** fNDs did not significantly reduce cell viability and induce senescence. **(A)** A549 or **(B)** HFL-1 cells were left treated with or without fNDs (0.1–100 µg/mL for 48 h). The cell viability was determined by MTT assay. Results were obtained from 4 independent experiments. The bars represent mean  $\pm$  SE. **(C)** The cell senescence after treatment with 0–50 µg/mL fNDs or MG132 (5 µM for 48 h; Calbiochem, 474790) in A549 cells was analyzed by the senescence-dependent GLB1/ $\beta$ -galactosidase activity staining (Cell Signaling, 9680). Blue color in the boxed regions indicates the senescent cells. **(D)** Quantification of senescent cells by counting cell number under an optical microscope. Results were obtained from 3 separate independent experiments. MG132 is a senescence inducer as a positive control.

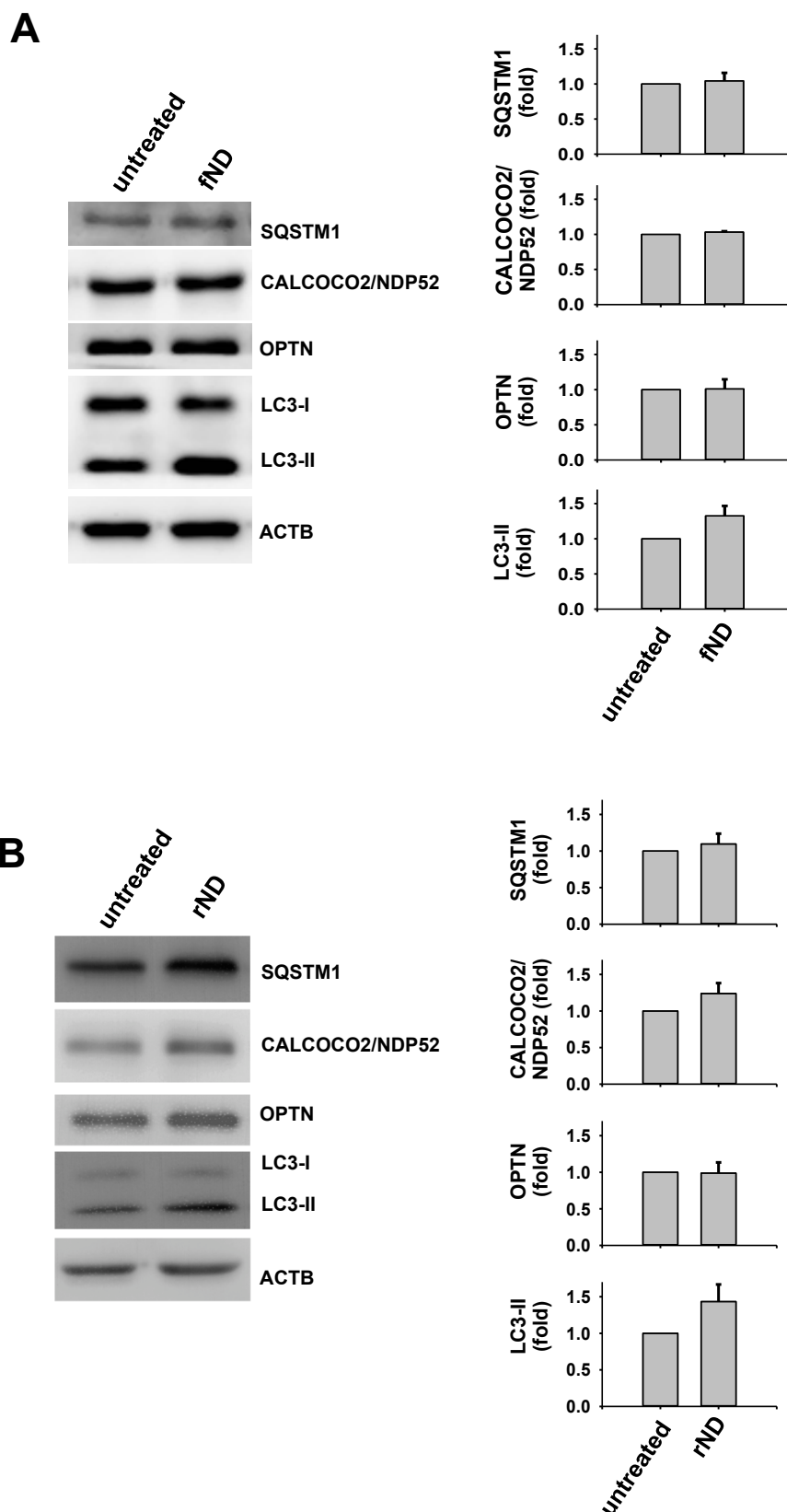


**Figure S25.** The protein expression of autophagy proteins after treatment with NDs. **(A)** A549 cells were left untreated or treated with fNDs (50  $\mu\text{g}/\text{mL}$  for 24 h). **(B)** A549 cells were left untreated or treated with rNDs (50  $\mu\text{g}/\text{mL}$  for 24 h). At the end of treatments, the total protein extracts were collected for western blot analyses using specific antibodies for SQSTM1, CALCOCO2/NDP52, OPTN and LC3. ACTB/ $\beta$ -actin was as a loading control. The protein levels were quantified. The bars represent mean  $\pm$  SE. Results were obtained from 3 independent experiments.